

# Solar System. Angular Momentum. New Physics

Vladimir S. Netchitailo

Biolase Inc., Irvine, CA, USA

Email: v.netchitailo@sbcglobal.net

**How to cite this paper:** Netchitailo, V.S. (2019) Solar System. Angular Momentum. New Physics. *Journal of High Energy Physics, Gravitation and Cosmology*, 5, 112-139. <https://doi.org/10.4236/jhepgc.2019.51005>

**Received:** November 5, 2018

**Accepted:** December 15, 2018

**Published:** December 18, 2018

Copyright © 2019 by author and Scientific Research Publishing Inc.

This work is licensed under the Creative Commons Attribution International License (CC BY 4.0).

<http://creativecommons.org/licenses/by/4.0/>



Open Access

---

## Abstract

The most widely accepted model of Solar System formation, known as the Nebular hypothesis, does not solve the Angular Momentum problem—why is the orbital momentum of Jupiter larger than rotational momentum of the Sun? The present manuscript introduces a Rotational Fission model of creation and evolution of Macrostructures of the World (Superclusters, Galaxies, Extrasolar Systems), based on Overspinning Cores of the World's Macroobjects, and the Law of Conservation of Angular Momentum. The Hypersphere World-Universe model is the only cosmological model in existence that is consistent with this Fundamental Law.

## Keywords

Hypersphere World-Universe Model, Medium of the World, Fifth Fundamental Force, Dark Matter Particles, Macroobjects Structure, Rotational Fission, Law of Conservation of Angular Momentum, Dark Epoch, Light Epoch, Dark Matter Reactor, Solar Corona, Geocorona, Planetary Corona, Solar Wind

---

## 1. Introduction

This paper is based on the World-Universe Model (WUM) [1]. To be consistent with the Law of Conservation of Angular Momentum, WUM is modified as follows:

- Overspinning Dark Matter Cores of Superclusters are the main players of the World's Macrostructures creation and evolution;
- New Dark Matter particles, named Dions, with mass 0.2 eV compose Outer shells of Supercluster's Cores;
- Dions with an energy density of 68.8% of the total energy density of the World are responsible for the gravitational interaction. In the modified WUM, we came back to the standard neutrino cosmology;
- Proposed Fifth Fundamental force of Weak Interaction between Dark Matter

particles provides the integrity of Dark Matter Cores of all Macroobjects;

- Dions outer shells of Supercluster's Cores are growing up to the maximum mass (see Section 4) during Dark Epoch lasting from the Beginning of the World (14.2 billion years ago) for 0.4 billion years;
- Light Galaxies and Extrasolar Systems arise due to Rotational Fission of Overspinning Supercluster's Cores and annihilation of Dark Matter particles;
- Macrostructures of the World form from the top (superclusters) down to galaxies, extrasolar systems, planets, and moons. Formation of galaxies and stars is not a process that concluded ages ago; instead, it is ongoing in the Light Epoch;
- Light Epoch spans from 0.4 billion years up to the present Epoch (during 13.8 billion years). The Big Bang discussed in the standard cosmological model is, in our view, the transition from Dark Epoch to Light Epoch.

In Section 2 of this article, we present a short history of Solar System formation. In Section 3, we develop the mathematical model of overspinning spherical objects. In Section 4, we introduce a new Dark Matter fermion, named "Dion," and a Fifth Fundamental Force that is responsible for a Weak Interaction between Dark Matter particles. In Section 5, we develop a Model of the formation and evolution of Macrostructures of the World from the Beginning of the World up to the present Epoch: Superclusters, Galaxies, Extrasolar Systems, Planets and Moons. In Section 6, we discuss main characteristics of Solar System: role of Dark Matter Cores in the Sun and in the gravitationally-rounded objects; composition of Corona, Geocorona, and Planetary Coronas; Solar wind; Planets activities and other features. In the Conclusion we postulate the principal role of Angular Momentum and Dark Matter in Cosmological theories of the World.

## 2. Short History of Solar System Formation

The most widely accepted model of Solar System formation, known as the Nebular hypothesis, was first proposed in 1734 by Emanuel Swedenborg [2], [3] and later elaborated and expanded upon by Immanuel Kant in 1755 in his "Universal Natural History and Theory of the Heavens" [4].

**Nebular hypothesis** maintains that 4.6 billion years ago, the Solar System formed from the gravitational collapse of a giant molecular cloud, which was light years across. Most of the mass collected in the Centre, forming the Sun; the rest of the mass flattened into a protoplanetary disc, out of which the planets and other bodies in the Solar System formed.

The Nebular hypothesis is not without its critics. In his "The Wonders of Nature", Vance Ferrell outlined the following counter-arguments [5]:

- It contradicts the obvious physical principle that gas in outer space never coagulates; it always spreads outward;
- Each planet and moon in solar system has unique structures and properties. How could each one be different if all of them came from the same nebula;
- A full 98 percent of all the angular momentum in the solar system is concen-

trated in the planets, yet a staggering 99.8 percent of all the mass in our Solar system is in our Sun;

- Jupiter itself has 60 percent of the planetary angular motion. Evolutionary theory cannot account for this. This strange distribution was the primary cause of the downfall of the Nebular hypothesis;
- There is no possible means by which the angular momentum from the Sun could be transferred to the planets. Yet this is what would have to be done if any of the evolutionary theories of Solar System origin are to be accepted. Speaking of the mass-angular momentum problem, Bergamini says: "*A theory of evolution that fails to account for this peculiar fact is ruled out before it starts*" [David Bergamini, *The Universe*, p. 93].

**Lunar origin fission hypothesis** was proposed by George Darwin in 1879 to explain the origin of the Moon by rapidly spinning Earth, on which equatorial gravitative attraction was nearly overcome by centrifugal force [6]. Donald U. Wise made a detailed analysis of this hypothesis in 1966 and concluded that "*it might seem prudent to include some modified form of rotational fission among our working hypothesis*" [7].

**Solar fission theory** was proposed by Louis Jacot in 1951 [8]. L. Jacot stated that:

- The planets were expelled from the Sun one by one from the equatorial bulge caused by rotation;
- One of these planets shattered to form the asteroid belt;
- The moons and rings of planets were formed from the similar expulsion of material from their parent planets.

Tom Van Flandern further extended this theory in 1993 [9]. Flandern proposed that planets were expelled from the Sun in pairs at different times. Six original planets exploded to form the rest of the modern planets. It solves several problems the standard model does not:

- If planets fission from the Sun due to overspin while the proto-Sun is still accreting, this more easily explains how 98% of the solar system's angular momentum ended up in the planets;
- It solves the mystery of the dominance of prograde rotation for these original planets since they would have shared in the Sun's prograde rotation at the outset;
- It also explains coplanar and circular orbits;
- It is the only model that explains the twinning of planets (and moons) and difference of planet pairs because after each planet pair is formed in this way, it will be some time before the Sun and extended cloud reach another overspin condition.

The outstanding issues of the Solar fission are:

- It is usually objected that tidal friction between a proto-planet and a gaseous parent, such as the proto-Sun, ought to be negligible because the gaseous parent can reshape itself so that any tidal bulge has no lag or lead, and therefore transfers no angular momentum to the proto-planet;
- There would exist no energy source to allow for planetary explosions.

- Neither L. Jacot nor T. Van Flarendern proposed an origin for the Sun itself. It seems that they followed the standard Nebular hypothesis of formation of the Sun.

In this work, we will concentrate on furthering the Solar Fission theory.

Let's consider rotational and orbital angular momentum of all gravitationally-rounded objects in the Solar system, from Mimas, a small moon of Saturn ( $3.75 \times 10^{19}$  kg), to the Sun itself ( $2 \times 10^{30}$  kg). Their angular momenta are presented in **Table 1**.

From the point of view of Fission model, the prime object is transferring some of its rotational momentum to orbital momentum of the satellite. It follows that the rotational momentum of the prime object should exceed the orbital momentum of its satellite.

From **Table 1** we see that orbital momenta of most satellites are indeed substantially smaller than the rotational momenta of their prime objects, with three exceptions (explored in Section 6):

- The rotational momentum of the Sun is smaller than Jupiter's, Saturn's, Uranus's, and Neptune's orbital momentum;
- The rotational momentum of the Earth is substantially smaller than Moon's orbital momentum;
- The rotational momentum of Pluto is considerably smaller than Charon's orbital momentum.

In Section 5 we will address the origins of these angular momenta.

### 3. Rotational Angular Momentum of Overspinning Objects

Let's calculate rotational angular momentum for an overspinning spherical object  $L_{rot}$ . It can be found according to the following equation:

$$L_{rot} = I\omega$$

where  $I$  is momentum of inertia and  $\omega$  is angular speed. Let's assume that a spherical object has a linear density distribution  $\rho$ :

$$\rho = \rho_{max} - (\rho_{max} - \rho_{min}) \frac{r}{R} = \rho_{max} \left[ 1 - (1 - \delta) \frac{r}{R} \right]$$

where  $\rho_{min}$  and  $\rho_{max}$  are values of density at the center and the edge of the object,  $R$  is its radius, and  $\delta$  is the density ratio:

$$\delta = \frac{\rho_{min}}{\rho_{max}}$$

Then mass  $M$  of the object is:

$$M = \frac{4\pi R^3}{3} \frac{\rho_{max}}{4} (1 + 3\delta)$$

and momentum of inertia  $I$  is:

$$I = 0.4 \times \frac{4\pi R^5}{3} \frac{\rho_{max}}{6} (1 + 5\delta) = 0.4 \times \frac{2}{3} MR^2 \frac{1 + 5\delta}{1 + 3\delta}$$

**Table 1.** Rotational and orbital angular momentum of gravitationally-rounded objects of the Solar System.

	Rotational Momentum (J s)	Orbital Momentum (J s)
<b>Sun</b>	1.10E+42	
<b>Mercury</b>	9.75E+29	9.15E+38
<b>Venus</b>	2.13E+31	1.85E+40
<b>Earth</b>	7.09E+33	2.66E+40
<b>Moon</b>	2.36E+29	2.89E+34
<b>Mars</b>	2.10E+32	3.53E+39
<b>Jupiter</b>	6.83E+38	1.93E+43
<b>Io</b>	4.84E+30	6.53E+35
<b>Europa</b>	9.68E+29	4.42E+35
<b>Ganimede</b>	4.18E+30	1.72E+36
<b>Callisto</b>	1.09E+30	1.66E+36
<b>Saturn</b>	1.35E+38	7.82E+42
<b>Mimas</b>	4.55E+25	9.96E+31
<b>Enceladus</b>	1.46E+26	3.25E+32
<b>Tethys</b>	2.70E+27	2.06E+33
<b>Dione</b>	3.67E+27	4.14E+33
<b>Rhea</b>	8.67E+27	1.03E+34
<b>Titan</b>	1.63E+30	9.16E+35
<b>Lapetus</b>	3.58E+26	2.10E+34
<b>Uranus</b>	2.30E+36	1.70E+42
<b>Miranda</b>	7.54E+25	5.67E+31
<b>Ariel</b>	5.22E+27	1.42E+33
<b>Umbriel</b>	2.88E+27	1.49E+33
<b>Titania</b>	7.28E+27	5.57E+33
<b>Oberon</b>	3.78E+27	5.54E+33
<b>Neptune</b>	2.72E+36	2.50E+42
<b>Triton</b>	1.94E+29	3.33E+34
<b>Pluto</b>	8.42E+28	3.66E+38
<b>Charon</b>	2.52E+27	5.32E+30
<b>Ceres</b>	1.62E+28	6.96E+36
<b>Haumea</b>	4.65E+29	1.18E+38
<b>Eris</b>	6.05E+29	6.12E+38

In case of spherical objects with homogeneous density,  $\delta = 1$ , then momentum of inertia  $I$  is simply

$$I = 0.4 \times MR^2$$

In **Table 1**, we assumed homogeneous density when calculating the rotational momentum  $L_{rot}$  of gravitationally-rounded objects. When the density differential is large (which is the case of the Sun, discussed in Section 5),  $\delta \ll 1$ , the momentum of inertia  $I$  reduces to:

$$I = 0.4 \times \frac{2}{3} MR^2$$

It is worth noting that the linear approximation of density distribution is good enough when calculating the rotational angular momentum  $L_{rot}$ . In case of non-linear density distributions  $L_{rot}$  will not change substantially.

For overspinning spherical objects, the angular velocity equals to:

$$\omega = \frac{v_{esc}}{R} = \frac{(2GM/R)^{0.5}}{R} = \frac{(2GM)^{0.5}}{R^{1.5}}$$

where  $v_{esc}$  is an escape velocity of the object and  $G$  is a gravitational parameter. Then, the rotational angular momentum of overspinning objects equals to:

$$L_{rot} = \frac{4\sqrt{2}}{15} \frac{1+5\delta}{1+3\delta} G^{0.5} M^{1.5} R^{0.5}$$

In accordance with WUM, parameters  $G$ ,  $M$ ,  $R$  for Macroobjects Cores are time-varying:  $G \propto \tau^{-1}$ ,  $M \propto \tau^{3/2}$  and  $R \propto \tau^{1/2}$ , where  $\tau$  is a cosmological time. It follows that the rotational angular momentum of Cores is proportional to:

$$L_{rot} \propto \tau^2$$

Let's introduce Age parameter  $\theta_F$  that is a ratio of cosmological time of Core fission  $\tau_F$  to the age of the World in present Epoch  $A_W$ :  $\theta_F = \tau_F / A_W$ . Finally, for  $L_{rot}$  at the time of Core fission we obtain the following equation:

$$L_{rot} = \frac{4\sqrt{2}}{15} \frac{1+5\delta}{1+3\delta} G^{0.5} M^{1.5} R^{0.5} \theta_F^2 \quad (3.1)$$

where for parameters  $G$ ,  $M$ ,  $R$  we use their values in the present Epoch. In the next Section we discuss the nature of overspinning spherical Cores of Macroobjects.

#### 4. Macroobjects Cores Made up of Dark Matter Particles

According to WUM, Macrostructures of the World (Superclusters, Galaxies, Extrasolar Systems) have Nuclei made up of Dark Matter Fermions (DMFs) [10]. In the Dark Epoch from the Beginning of the World during 0.4 billion years these Nuclei are surrounded by Shells composed of Dark Matter Particles (DMPs).

The Shells envelope one another, like a Russian doll. The lighter a DMP, the greater the radius and the mass of its shell. Innermost shells are the smallest and are made up of heaviest particles; outer shells are larger and consist of lighter particles [11].

WUM postulates that masses of DMPs are proportional to a basic unit of mass

$m_0$  multiplied by different exponents of  $\alpha$  [12]:

- DMF1 (fermion):  $m_{DMF1} = \alpha^{-2}m_0$
- DMF2 (fermion):  $m_{DMF2} = \alpha^{-1}m_0$
- DIRAC (boson):  $m_{DIRAC} = \alpha^0m_0$
- ELOP (boson):  $m_{ELOP} = \frac{2}{3}\alpha^1m_0$
- DMF3 (fermion):  $m_{DMF3} = \alpha^2m_0$
- DMF4 (fermion):  $m_{DMF4} = \alpha^4m_0$

where  $\alpha$  is Sommerfeld's constant and is, in fact, the ratio of electron mass  $m_e$  to the basic unit of mass  $m_0$ :  $\alpha = m_e/m_0$  and  $m_0$  equals to:  $m_0 = h/ac$ , where  $h$  is Planck constant,  $c$  is the electrodynamic constant and  $a$  is the basic unit of length:  $a = \alpha\lambda_e$  and  $\lambda_e$  is Compton wavelength of an electron:  $\lambda_e = h/m_e c$  [12].

The values of Dark Matter Fermion masses DMF1, DMF2, DMF3 fall into the ranges estimated in literature for neutralinos, WIMPs, and sterile neutrinos respectively [10].

DMF1, DMF2 and DMF3 are Majorana fermions, which partake in the annihilation interaction with strength equals to  $\alpha^{-2}$ ,  $\alpha^{-1}$ , and  $\alpha^2$  respectively. The signatures of DMPs annihilation with expected masses of 1.3 TeV; 9.6 GeV; 3.7 keV are found in spectra of the diffuse gamma-ray background and the emission of various macroobjects in the World [10]. **Table 2** describes the parameters of Fermionic Compact Stars (FCSs) made up of different DMFs in the present Epoch.

The calculated parameters of the shells show that [11]:

- Nuclei made of annihilating DMF1 or DMF2 compose Cores of stars in extrasolar systems;
- Shells of annihilating DMF3 around Nuclei made up of annihilating DMF1 or DMF2 make up Cores of galaxies;
- Shells of DMF4 around Nuclei made up of annihilating DMF1, DMF2, DMF3 compose Cores of superclusters.

Fermionic Compact Stars have the following properties:

- The maximum potential of interaction  $U_{max}$  between any particle or macroobject and FCS made up of any fermions does not depend on the nature of fermions;

**Table 2.** Parameters of FCSs made up of different DMFs in the present Epoch.

Fermion	Fermion mass $m_f, \text{MeV}/c^2$	Macroobject mass $M_{max}, \text{kg}$	Macroobject radius $R_{min}, \text{m}$	Macroobject density $\rho_{max}, \text{kg}/\text{m}^3$
DMF1	$1315 \times 10^3$	$1.9 \times 10^{30}$	$8.6 \times 10^3$	$7.2 \times 10^{17}$
DMF2	9596	$1.9 \times 10^{30}$	$8.6 \times 10^3$	$7.2 \times 10^{17}$
DMF3	$3.73 \times 10^{-3}$	$1.2 \times 10^{41}$	$5.4 \times 10^{14}$	$1.8 \times 10^{-4}$
DMF4	$2 \times 10^{-7}$	$4.2 \times 10^{49}$	$1.9 \times 10^{23}$	$1.5 \times 10^{-21}$

$$U_{\max} = \frac{GM_{\max}}{R_{\min}} = \frac{c^2}{6}$$

- The maximum orbit velocity  $v_o$  does not depend on the nature of fermions;

$$v_o = \sqrt{\frac{GM_{\max}}{R_{\min}}} = \frac{c}{\sqrt{6}}$$

- The minimum radius of FCS made of any fermion equals to three Schwarzschild radii  $R_{SH}$  and does not depend on the nature of the fermion;

$$R_{\min} = 3R_{SH}$$

- FCS density does not depend on  $M_{\max}$  and  $R_{\min}$  and does not change in time while  $M_{\max} \propto \tau^{3/2}$  and  $R_{\min} \propto \tau^{1/2}$ .

**Fifth Fundamental Force.** Dark Matter (DM) is among the most important open problems in both cosmology and particle physics. The widely discussed models for nonbaryonic DM are based on the Cold Dark Matter hypothesis, and corresponding particles are commonly assumed to be Weakly Interacting Massive Particles (WIMPs).

According to Wikipedia,

*A WIMP is a new elementary particle which interacts via gravity and any other force (or forces), potentially not part of the standard model itself, which is as weak as or weaker than the weak nuclear force, but also non-vanishing in its strength.*

It follows that a Fifth Fundamental force needs to exist, providing interaction between DMPs with strength far exceeding gravity, and with range considerably greater than that of the weak nuclear force.

According to WUM, strength of gravity is characterized by gravitational parameter

$$G = G_0 Q^{-1}$$

where  $G_0 = \frac{a^2 c^4}{8\pi h c}$  is an extrapolated value of  $G$  at the Beginning of the World and dimensionless time-varying quantity  $Q$  is a measure of the age of the World:

$$Q = \tau/t_0$$

where  $t_0$  is a basic unit of time that equals to:

$$t_0 = a/c = 5.9059674 \times 10^{-23} \text{ s}$$

$Q$  in the present Epoch equals to [1]:

$$Q = 0.759972 \times 10^{40}$$

The range of the gravity equals to the size of the World  $R$ :

$$R = aQ = 1.34558 \times 10^{26} \text{ m}$$

In WUM, weak interaction is characterized by the parameter  $G_W$  :

$$G_W = G_0 Q^{-1/4}$$

which is about 30 orders of magnitude greater than  $G$ . The range of the weak interaction  $R_W$  in the present Epoch equals to:

$$R_W = aQ^{1/4} = 1.65314 \times 10^{-4} \text{ m} \quad (4.1)$$

that is much greater than the range of the weak nuclear force that is around  $\sim 10^{-16} - 10^{-17} \text{ m}$ .

Calculated concentration of Dions  $n_D$  in the largest shell with the density  $\rho_D \cong 1.5 \times 10^{-21} \text{ kg/m}^3$ :

$$n_D \cong 4.2 \times 10^{15} \text{ m}^{-3}$$

shows that a distance between particles is around  $\sim 10^{-5} \text{ m}$ , which is much smaller than  $R_W$ . Thus, the weak interaction between DMPs will provide integrity of DM shells.

It is worth noting that the critical density of the World in the present Epoch equals to [1]:

$$\rho_{cr} = 3\rho_0 Q^{-1} \cong 8.9 \times 10^{-27} \text{ kg/m}^3$$

which is about 5 orders of magnitude smaller than  $\rho_D$  ( $\rho_0 = \frac{h/c}{a^4}$  is a basic unit of density). Distance between particles in the Medium of the World is around  $\sim 10^{-3} \text{ m}$  that is larger than  $R_W$ .

## 5. Beginning of the World. Dark Epoch. Rotational Fission. Light Epoch

**Beginning of the World.** Before the Beginning there was nothing but an Eternal Universe. About 14.2 billion years ago the World was started by a fluctuation in the Eternal Universe, and the Nucleus of the World, which is a four-dimensional 4-ball, was born. An extrapolated Nucleus radius at the Beginning was equal to  $a$  that is chosen to fit the Age of the World. The 3D World is a hypersphere that is the surface of a 4-ball Nucleus. All points of the hypersphere are equivalent; there are no preferred centers or boundary of the World [1] [12].

**Expansion.** The 4-ball is expanding in the Eternal Universe, and its surface, the hypersphere, is likewise expanding so that the radius of the Nucleus  $R$  is increasing with speed  $c$  that is the gravitoelectrodynamic constant, for the absolute cosmological time  $\tau$  from the Beginning and equals to  $R = c\tau$ . The expansion of the Hypersphere World can be understood by the analogy with an expanding 3D balloon: imagine small enough “flat” observer residing in a curved flatland on the surface of a balloon; as the balloon is blown up, the distance between all neighboring points grows; the two-dimensional world grows but there is no preferred center [1] [12].

**Creation of Matter.** The surface of the 4-ball is created in a process analogous to sublimation. It is a well-known endothermic process that occurs when surfaces are intrinsically more energetically favorable than the bulk of a material, and hence there is a driving force for surfaces to be created. Continuous creation of matter is the result of a similar process. Matter arises from the fourth spatial di-

mension. The Universe is responsible for the creation of Matter. Dark Matter particles carry new Matter in the World. Creation of Matter is a direct consequence of expansion. Creation of DM occurs homogeneously in all points of the hypersphere World [1] [12].

**Dark Epoch** started at the Beginning of the World and lasted for about 0.4 billion years. Hypersphere WUM is a classical model. According to the model, classical notions can be introduced only when the very first ensemble of particles was created at the cosmological time  $\tau_q = t_0 \alpha^{-2} \cong 10^{-18}$  s [1]. The World at cosmological times less than  $10^{-18}$  s is best described by Quantum mechanics. The value of the parameter  $Q$  at that time was:  $Q_q = \alpha^{-2}$ ; a size of the World  $R_q$  was  $a \times \alpha^{-2} = 2\pi a_B$  ( $a_B$  is Bohr radius) and a total mass of the World:

$$M_W = 6\pi^2 m_0 \times Q^2 = 6\pi^2 m_0 \alpha^{-4} \cong 2.6 \times 10^{-18} \text{ kg}$$

At time  $\tau \gg \tau_q$  density fluctuations could happen in the Medium of the World filled out with DMF1, DMF2, DIRACs, ELOPs, DMF3 and DMF4. The heaviest DMF1 with mass  $m_{DMF1} = m_0 \alpha^{-2}$  could collect into a cloud of radius  $R_{cl}$  with distance between them equals to  $R_W = aQ^{1/4}$ . As the result of the weak interaction, clumps of DMF1 will arise with density  $\rho_{cl} = \rho_0 \alpha^{-2} \times Q^{-3/4}$ , volume  $V_{cl}$  and mass  $M_{cl}$ :

$$M_{cl} = \rho_0 \alpha^{-2} V_{cl} \times Q^{-3/4}$$

Considering the analogy between electromagnetic and gravitoelectromagnetic fields [1], we can write the following equation for the minimum product of objects masses to exert gravity on one another:

$$m_{DMF1} M_{cl} = m_0^2 \alpha^{-4} a^{-3} V_{cl} \times Q^{-3/4} = 2m_0^2 \times Q$$

The volume of a clump  $V_{cl}$  then equals to

$$V_{cl} = 2\alpha^4 a^3 \times Q^{7/4}$$

and mass of a clump  $M_{cl}$  is:

$$M_{cl} = 2m_0 \alpha^2 \times Q$$

A well-elaborated classical model can be introduced when the cosmological time was  $\tau_{cl} = t_0 \alpha^{-8} \cong 7 \times 10^{-6}$  s. Taking the value of the parameter  $Q_{cl} = \alpha^{-8}$  we get

$$M_{cl} = 2m_0 \alpha^{-6} \cong 1.6 \times 10^{-15} \text{ kg}$$

$$R_{cl} = a(3/2\pi)^{1/3} \alpha^{-10/3} \cong 1.8 \times 10^{-7} \text{ m}$$

$$\rho_{cl} = \rho_0 \alpha^4 \cong 6.4 \times 10^4 \text{ kg/m}^3$$

$$R_W^{cl} = a \times \alpha^{-2} \cong 3.3 \times 10^{-10} \text{ m}$$

At that time, mass  $M_{World}$  and size  $R_{World}$  of the World were

$$M_{World} = 6\pi^2 m_0 \times Q^2 \cong 10^8 \text{ kg}$$

$$R_{World} = a \times \alpha^{-8} \cong 2 \times 10^3 \text{ m}$$

Analogous calculations for DMF2 produce the following results for clump mass  $M'_{cl}$  and density  $\rho'_{cl}$ :

$$M'_{cl} = 2m_0\alpha^{-7} \cong 2.2 \times 10^{-13} \text{ kg}$$

$$\rho'_{cl} = \rho_0 a^5 \cong 4.7 \times 10^2 \text{ kg/m}^3$$

Larger clumps will attract smaller clumps and DMPs and initiate a process of expanding the DM Core to the maximum mass of the shell made up of Dions. Considering the Age parameter  $\theta_{0.4} \cong 1/36$  and dependence of Core mass  $M_{\text{Core}} \propto \tau^{3/2}$  and Core size  $R_{\text{Core}} \propto \tau^{1/2}$ , we obtain  $M_{\text{Core}}^{0.4} = 2.3 \times 10^{47} \text{ kg}$  and  $R_{\text{Core}}^{0.4} = 3.2 \times 10^{22} \text{ m}$  at the end of Dark Epoch (0.4 billion years). This is the Core of Supercluster. Considering the total mass of the World at that time  $M_{\text{tot}}^{0.4}$ :

$$M_{\text{tot}}^{0.4} = 6\pi^2 m_0 \times Q_{0.4}^2 = 3.3 \times 10^{50} \text{ kg}$$

we estimate the number of Supercluster Cores to be around  $\sim 10^3$ . In our opinion, all Supercluster Cores had undergone rotational fission at approximately the same cosmological time.

**Rotational Fission.** Local Supercluster is a mass concentration of galaxies containing the Local Group, which in turn contains the Milky Way galaxy. At least 100 galaxy groups and clusters are located within its diameter of 110 million light-years.

Let's calculate the rotational angular momentum  $L_{\text{rot}}^{LSC}$  of Local Supercluster Core (LSC) before rotational fission based on the Equation (3.1) and parameters of Dion shell (see **Table 2**) with the Age parameter  $\theta_{0.4} \cong 1/36$ :

$$L_{\text{rot}}^{LSC} = 3.7 \times 10^{77} \text{ J}\cdot\text{s}$$

Milky Way (MW) is gravitationally bounded with Local Supercluster (LS) [13]. Let's compare  $L_{\text{rot}}^{LSC}$  with an orbital momentum of Milky Way  $L_{\text{orb}}^{MW}$  calculated based on the distance of 65 million light years from LSC and orbital speed of about 400 km/s [13]:

$$L_{\text{orb}}^{MW} = 2.5 \times 10^{71} \text{ J}\cdot\text{s}$$

It means that as the result of rotational fission of LS Core, approximately  $\sim 10^6$  galaxies like Milky Way could be generated at the same time. Considering that the number density of galaxies in the LS falls off with the square of the distance from its center near the Virgo Cluster, and the location of MW on the outskirts of the LS [14], the actual number of created galaxies could be much larger.

Analogous calculations for Milky Way Core (MWC) based on parameters of DMF3 shell produce the following value of rotational angular momentum  $L_{\text{rot}}^{MWC}$ :

$$L_{\text{rot}}^{MWC} = 2.4 \times 10^{60} \text{ J}\cdot\text{s}$$

which far exceeds the orbital momentum of the Solar System  $L_{\text{orb}}^{SS}$  calculated based on the distance from the galactic center of 26,400 light years and orbital speed of about 220 km/s:

$$L_{\text{orb}}^{SS} = 1.1 \times 10^{56} \text{ J}\cdot\text{s} \tag{5.1}$$

As the result of rotational fission of Milky Way's Core 13.8 billion years ago, approximately  $\sim 10^4$  Extrasolar systems like Solar System could be created at the same time. Considering that MW has grown inside out (in the present Epoch, most old stars can be found in the middle, more recently formed ones on the outskirts [15]), the number of generated Extrasolar systems could be much larger.

Extrasolar system Cores can give birth to planet cores, and they can generate cores of moons by the same Rotational Fission mechanism (see next Section).

The mass-to-light ratio of the Local Supercluster is about 300 times larger than that of the Solar ratio. Similar ratios are obtained for other superclusters [16]. These facts support the rotational fission mechanism proposed above.

In 1933, Fritz Zwicky investigated the velocity dispersion of Coma cluster and found a surprisingly high mass-to-light ratio ( $\sim 500$ ). He concluded: *if this would be confirmed, we would get the surprising result that dark matter is present in much greater amount than luminous matter* [17]. These ratios are one of the main arguments in favor of presence of large amounts of Dark Matter in the World.

**Light Epoch** spans from 0.4 billion years up to the present Epoch (during 13.8 billion years). According to WUM, Cores of all Macroobjects (MO) of the World (Superclusters, Galaxies, Extrasolar systems) possess the following properties:

- Their Nuclei are made up of DMFs and contain other particles, including Dark Matter and baryonic matter, in shells surrounding the Nuclei;
- DMPs are continuously absorbed by Cores of all MOs. Light Matter (about 7.2% of the total Matter in the World) is a product of DMPs annihilation. Light Matter (LM) is re-emitted by Cores of MOs continuously;
- Nuclei and shells are growing in time: size  $\propto \tau^{1/2}$ ; mass  $\propto \tau^{3/2}$  and rotational angular momentum  $\propto \tau^2$ , until they reach the critical point of their stability, at which they detonate. Satellite cores and their orbital  $L_{orb}$  and rotational  $L_{rot}$  angular momenta released during detonation are produced by Over-spinning Core (OC). The detonation process does not destroy OC; it's rather gravitational hyper-flares;
- Size, mass, composition,  $L_{orb}$  and  $L_{rot}$  of satellite cores depend on local density fluctuations at the edge of OC and cohesion of the outer shell. Consequently, the diversity of satellite cores has a clear explanation.

This is a description of Gravitational Bursts (GBs) analogous to the description of Gamma Ray Bursts (GRBs) and Fast Radio Bursts (FRBs) [11]. In frames of WUM, the repeating GBs can be explained the following way:

- As the result of GB, the OC loses a small fraction of its mass and a large part of its rotational angular momentum;
- After GB the Core absorb new DMPs increasing its mass  $\propto \tau^{3/2}$  and growing up  $L_{rot}$  much faster  $\propto \tau^2$  until the next critical point of its stability at which it detonates again;
- Afterglow of GBs is a result of processes developing in the Nuclei and shells after detonation. In case of Extrasolar systems, a star wind is the afterglow of

star detonation: star Core absorbs new DMPs, increase its mass  $\propto \tau^{3/2}$  and gets rid of extra  $L_{rot}$  by star wind particles.

In frames of the developed Rotational Fission model it is easy to explain hyper-runaway stars unbound from the Milky Way with speeds of up to  $\sim 700$  km/s [18]: they were launched by overspinning Core of the Large Magellanic Cloud with the speed higher than the escape velocity.

C. J. Clarke *et al.* observed CI Tau, a young 2 million years old star. CI Tau is located about 500 light years away in a highly-productive stellar 'nursery' region of the galaxy. They discovered that the Extrasolar System contains four gas giant planets that are only 2 million years old [19], amount of time that is too short for formation of gas giants according to prevailing theories.

In frames of the developed Rotational Fission model, this discovery can be explained by Gravitational Burst of the overspinning Core of the Milky Way two million years ago, which gave birth to CI Tau system with all planets generated at the same time.

To summarize,

- The rotational fission of macroobject cores is the most probable process that can generate satellite cores with large orbital momenta in a very short time;
- Macrostructures of the World form from the top (superclusters) down to galaxies, extrasolar systems, planets, and moons;
- Gravitational waves can be a product of rotational fission of overspinning Macroobject Cores;
- Hypersphere World-Universe model can serve as a basis for Transient Gravitational Astrophysics.

In the next Section we discuss main characteristics of Solar System considering the developed mechanism of Rotational Fission.

## 6. Solar System

**Angular momentum.** The Solar system was born 4.6 billion years ago as the result of the repeating Gravitational burst of Milky Way's Core. At that time, Age parameter  $\theta_{9,6}$  equaled about  $\cong 2/3$ , and the rotational angular momentum of the Core  $L_{rot}^{MWC}$  was much larger than  $L_{orb}^{SS}$  (see Equation (5.1)):

$$L_{rot}^{MWC} = 1.4 \times 10^{63} \text{ J} \cdot \text{s}$$

At that time, the Galactic Core could generate approximately  $\sim 10^7$  Extrasolar systems like the Solar system. Considering that Jupiter's orbital momentum is about 60% of the total angular momentum of Solar System  $L_{tot}^{SS}$ , we obtain

$$L_{tot}^{SS} \cong 3.2 \times 10^{43} \text{ J} \cdot \text{s} \quad (6.1)$$

Let's calculate parameters of the Sun's Core necessary to provide this angular momentum. Substituting mass  $M_{Sun} = 2 \times 10^{30}$  kg and radius  $R_{Sun} = 7 \times 10^8$  m and using Equation (3.1) we obtain

$$L_{rot}^{Sun} = 1.1 \times 10^{44} \text{ J} \cdot \text{s}$$

which is 3.3 times greater than  $L_{tot}^{SS}$ . It follows that the Sun's Core can be small-

er.

Let's consider the structure of the Sun. According to the standard Solar model it has:

- Core that extends from the center to about 20% - 25% of the solar radius, contains 34% of the Sun's mass with density  $\rho_{\max} = 1.5 \times 10^5 \text{ kg/m}^3$  and  $\rho_{\min} = 2 \times 10^4 \text{ kg/m}^3$ . It produces all Sun's energy;
- Radiative zone from the Core to about 70% of the solar radius with density  $\rho_{\max} = 2 \times 10^4 \text{ kg/m}^3$  and  $\rho_{\min} = 2 \times 10^2 \text{ kg/m}^3$  in which convection does not occur and energy transfer occurs by means of radiation;
- Core and Radiative zone contain practically all Sun's mass [20].

In our opinion, the Sun has an Inner Core (Nucleus made up of DMF1) whose radius is 20–25% of the solar radius, and an Outer Core—the Radiative zone. We then calculate the Solar Core rotational angular momentum  $L_{rot}^{SC}$ :

$$L_{rot}^{SC} \cong 8.9 \times 10^{43} \text{ J} \cdot \text{s}$$

which is 2.8 times larger than the overall angular momentum of the Solar System (6.1).

Let's follow the same procedure for the Earth-Moon pair. Considering the mass of Earth  $M_{Earth} = 6 \times 10^{24} \text{ kg}$  and radius  $R_{Earth} = 6.4 \times 10^6 \text{ m}$  and using (3.1) ( $\theta_{9,6} \cong 2/3$  and  $\delta = 2.9/13.1$ ) we calculate  $L_{rot}^{Earth} = 6.6 \times 10^{34} \text{ J} \cdot \text{s}$  that is 2.3 times larger than the Moon's orbital momentum  $L_{orb}^{Moon} = 2.9 \times 10^{34} \text{ J} \cdot \text{s}$  (see **Table 1**).

Let's look at the structure of the Earth. According to the standard model it has:

- An inner core and an outer core that extend from the center to about 45% of the Earth radius with density  $\rho_{\max} = 1.3 \times 10^4 \text{ kg/m}^3$  and  $\rho_{\min} = 9.9 \times 10^3 \text{ kg/m}^3$ ;
- Lower mantle, spanning from the outer core to about 90% of the Earth radius (below 660 km) with density  $\rho_{\max} = 5.6 \times 10^3 \text{ kg/m}^3$  and  $\rho_{\min} = 4.4 \times 10^3 \text{ kg/m}^3$ ;
- Inner core, outer core, and lower mantle contain practically all of the Earth's mass [21].

Very little is known about the lower mantle apart from that it appears to be relatively seismically homogeneous. Outer core-lower mantle boundary has a sharp drop of density  $(9.9 \rightarrow 5.6) \times 10^3 \text{ kg/m}^3$  [21].

In our opinion, lower mantle is a part of the Earth's core. It could be significantly different 4.6 billion years ago, since during this time it was gradually filled with all chemical elements produced by Earth's core due to DMF1 annihilation. Considering the Earth's core (EC) with radius  $R_{core}^{Earth} = 5.7 \times 10^6 \text{ m}$  ( $\theta_{9,6} \cong 2/3$  and  $\delta = 4.4/13.1$ ), the rotational angular momentum equals to:

$$L_{rot}^{EC} = 6.5 \times 10^{34} \text{ J} \cdot \text{s}$$

which is 2.2 times larger than the orbital momentum of the Moon.

As for the Pluto-Charon pair, it is definitely a binary system. Charon was not

generated by Pluto's core; instead, they are two independent objects that happened to be bounded together by gravity.

**Earth's internal heat.** According to the standard model, the Earth's internal heat is produced mostly through radioactive decay. The major heat-producing isotopes within Earth are K-40, U-238, and Th-232 with half-lives of  $(1.25; 4.47; 14.0) \times 10^9$  year respectively, and with the calculated mean mantle concentrations of  $(36.9; 30.8; 124) \times 10^{-9} \frac{\text{kg isotope}}{\text{kg mantle}}$  respectively [22]. The mean global heat loss from Earth is 44.2 TW [23]. The Earth's Uranium has been thought to be produced in one or more supernovae over 6 billion years ago [24].

**Radiogenic decay** can be estimated from the flux of geoneutrinos that are emitted during radioactive decay. The KamLAND Collaboration combined precise measurements of the geoneutrino flux from the Kamioka Liquid-Scintillator Antineutrino Detector, Japan, with existing measurements from the Borexino detector, Italy. They found that decay of U-238 and Th-232 together contribute about 20 TW to the total heat flux from the Earth to space  $44.2 \pm 1.0$  TW. The neutrinos emitted from the decay of K-40 were below the limits of detection in their experiments but are known to contribute 4 TW. Based on the observations the KamLAND Collaboration made a conclusion *that heat from radioactive decay contributes about half of Earth's total heat flux* [25].

**Plutonium-244.** According to the Wikipedia article,

*Pu-244 has a half-life of 80 million years. Unlike other plutonium isotopes, Pu-244 is not produced in quantity by the nuclear fuel cycle, because it needs very high neutron flux environments. A nuclear weapon explosion can produce some Pu-244 by rapid successive neutron capture.*

Nevertheless, D. C. Hoffman *et al.* in 1971 obtained the first indication of Pu-244 present existence in Nature [26].

In our opinion, all chemical products of the Earth including isotopes K-40, U-238, Th-232, and Pu-244, are produced within the Earth as the result of DMF1 annihilation. They arrive in the Crust of the Earth due to convection currents in the mantle carrying heat and isotopes from the interior to the planet's surface [27].

**Gravitationally-rounded objects internal heat.** The analysis of Sun's heat for planets in Solar system yields the effective temperature of Earth of 255 K [28]. The actual mean surface temperature of Earth is 288 K [29]. The higher actual temperature of **Earth** is due to energy generated internally by the planet itself.

**Jupiter** radiates more heat than it receives from the Sun [30]. Giant planets like Jupiter are hundreds of degrees warmer than current temperature models predict. Until now, the extremely warm temperatures observed in Jupiter's atmosphere (about 970 degrees C [31]) have been difficult to explain, due to lack of a known heat source [12].

**Saturn** radiates 2.5 times more energy than it receives from the Sun [32]; **Uranus**—1.1 times [33]; **Neptune**—2.6 times [34].

The most fascinating result was obtained for the smallest gravitationally-rounded object—Mimas. **Figure 1** illustrates the unexpected and bizarre pattern of daytime temperatures found on it.

**Dark Matter Cores.** The following facts support the existence of DM Cores in Macroobjects:

- Fossat *et al.* found that Solar Core rotates  $3.8 \pm 0.1$  faster than the surrounding envelope [36];
- By analyzing the earthquake doublets, Zhang *et al.* concluded that the Earth's inner core is rotating faster than its surface by about 0.3 - 0.5 degrees per year [37];
- T. Guillot *et al.* found that a deep interior of Jupiter rotates nearly as a rigid body, with differential rotation decreasing by at least an order of magnitude compared to the atmosphere [38].

The fact that Macroobject Cores rotate faster than surrounding envelopes, despite high viscosity of the internal medium, is intriguing. WUM explains this phenomenon through absorption of DMPs by Cores. Dark Matter Particles supply not only additional mass ( $\propto \tau^{3/2}$ ), but also additional angular momentum ( $\propto \tau^2$ ). Cores irradiate products of annihilation, which carry away excessive angular momentum. The Solar wind is the result of this mechanism.

**WUM explanation.** The internal heating of all gravitationally-rounded objects of the Solar system is due to DMPs annihilation in their Nuclei made up of

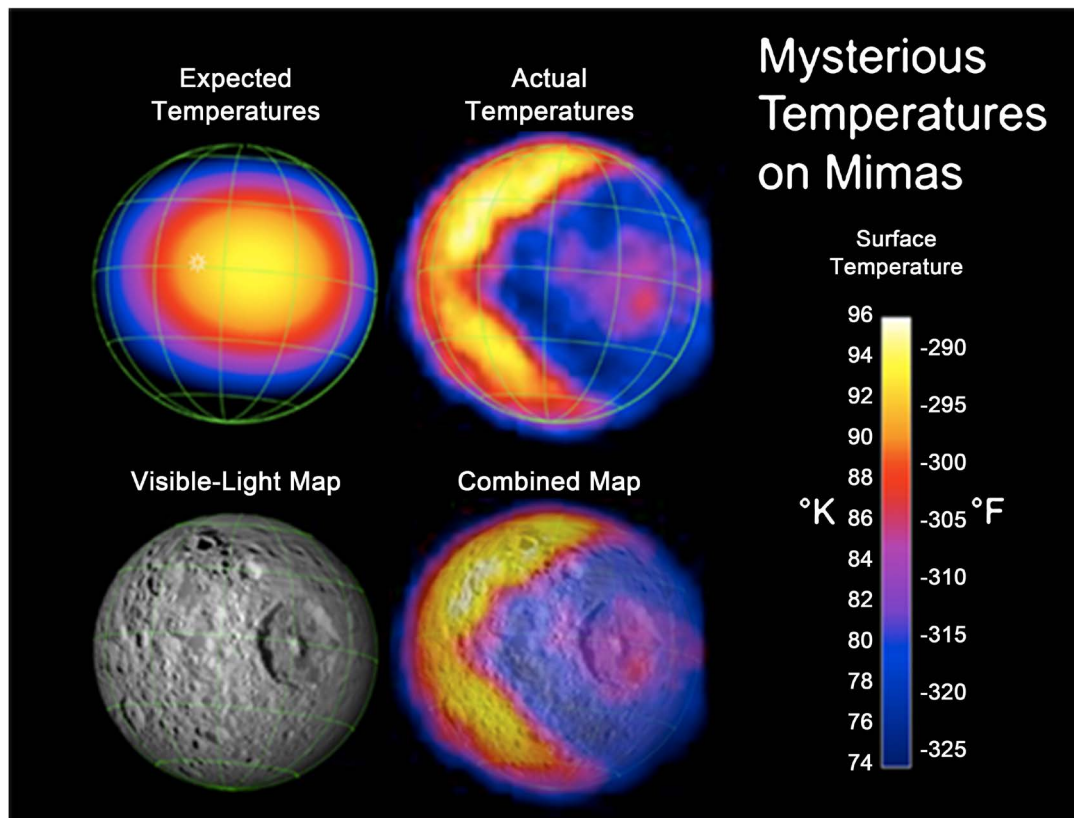


**Figure 1.** Mimas pattern of daytime temperatures. Adapted from [35].

DMF1 with mass 1.3 TeV (compare to proton mass: 938 MeV). The amount of energy produced due to this process is sufficiently high to heat up the objects. New DMF1 freely penetrate through the entire objects' envelope, get absorbed into the nucleus and support DMF1 annihilation continuously. Objects' nuclei are "DM Reactors" fueled by DMF1 [12].

In our opinion, all chemical elements, compositions, substances, rocks, etc. are produced by Macroobjects themselves as the result of DMPs annihilation. The diversity of all gravitationally-rounded objects of the Solar System is explained by their distance from the Sun, and the differences in their Cores (mass, size, composition).

The "DM Reactor" inside of all gravitationally-rounded objects (including Earth) provides sufficient energy for all geological processes on planets and satellites. All gravitationally-rounded objects in hydrostatic equilibrium, down to Mimas in Solar system, prove the validity of WUM [12].

**The evolution of the Sun.** By 1950s, stellar astrophysicists had worked out the physical principles governing the structure and evolution of stars [39]. According to these principles, the Sun's luminosity had to change over time, with the young Sun being about 30% less luminous than today [40] [41] [42] [43]. The long-term evolution of the bolometric solar luminosity  $L(\tau)$  as a function of cosmological time  $\tau$  can be approximated by a simple linear law:  $L(\tau) \propto \tau$  [39].

One of the consequences of WUM holds that all stars were fainter in the past. As their cores absorb new DM, size of MO cores  $R_{MO}$  and their luminosity  $L_{MO}$  are increasing in time:  $R_{MO} \propto \tau^{1/2}$  and  $L_{MO} \propto R_{MO}^2 \propto \tau$  respectively. Taking the age of the World  $A_W \cong 14.2$  Byr and the age of the solar system  $A_{SS} \cong 4.6$  Byr, it is easy to find that the young Suns' output was 67% of what it is today. Literature commonly refers to the value of 70% [42] [43]. This result supports the developed model of the structure and evolution of the Sun [39].

**Pioneer anomaly.** According to Fractal Cosmology, Macroobject Cores are surrounded by a transitional region. In this region, the density decreases rapidly to the point of the zero level of the fractal structure [44] characterized by radius  $R_f$  and density  $\rho_f$ , that satisfy the following equation for  $r \geq R_f$ :

$$\rho(r) = \frac{\rho_f R_f}{r} \quad (6.2)$$

According to Yu. Baryshev: *For a structure with fractal dimension  $D = 2$  the constant  $\rho_f R_f$  may be actually viewed as a new fundamental physical constant* [44]. In WUM, it is natural to connect this constant with a basic unit of energy density  $\sigma_0 = hc/a^3$ :

$$\rho_f R_f = 4\sigma_0/c^2 \quad (6.3)$$

The value of 4 above follows from the ratio for all MOs of the World: 1/3 of the total energy is in the central macroobject and 2/3 of the total energy is in the structure around it [10].

Wikipedia describes the so-called Pioneer anomaly as

*observed deviation from predicted accelerations of the Pioneer 10 and Pioneer 11 spacecraft after they passed about 20 astronomical units on their trajectories out of the Solar System. An unexplained force appeared to cause an approximately constant sunward acceleration of  $a_p = 8.74 \pm 1.33 \times 10^{-10} \text{ m/s}^2$  for both spacecraft. The magnitude of the Pioneer effect  $a_p$  is numerically quite close to the product of the speed of light  $c$  and the Hubble constant  $H_0$  hinting at cosmological connection.*

Let us calculate deceleration  $a_p$  at the distance  $r_p \gg R_f$  due to additional mass of the structure  $M_{FS} \propto r_p^2$  with the following equation for gravitational parameter in the present Epoch  $G = \frac{c^4}{8\pi\sigma_0 R_0}$  [10]:

$$a_p = \frac{GM_{FS}}{r_p^2} = \frac{c^4}{8\pi\sigma_0 R_0} \times \frac{8\pi\sigma_0}{c^2} \times \frac{c^2}{R_0} = cH_0 = 6.68 \times 10^{-10} \text{ m/s}^2$$

which is in good agreement with the experimentally measured value ( $R_0$  and  $H_0$  are the values of the World's size  $R$  and Hubble's parameter  $H$  at the present Epoch). It is important to notice that the calculated deceleration does not depend on  $r_p$  and equals to  $cH_0$  for all objects around the Macroobject at the distance  $r \gg R_f$ .

Mass of the structure around Sun  $M_V$  at distances  $R_V \gg R_f$  is:

$M_V = \frac{8\pi R_V^2 \sigma_0}{c^2}$ . At distance to Voyager 1:  $R_V \cong 1.8 \times 10^{13} \text{ m}$  [45], the structure mass is:  $M_V \cong 3.3 \times 10^{27} \text{ kg}$  that is  $\sim 0.15\% M_{Sun}$ .

**Structure of the Solar atmosphere.** Let's take a look at the structure of Solar atmosphere, its density and temperature depicted in **Figure 2**.

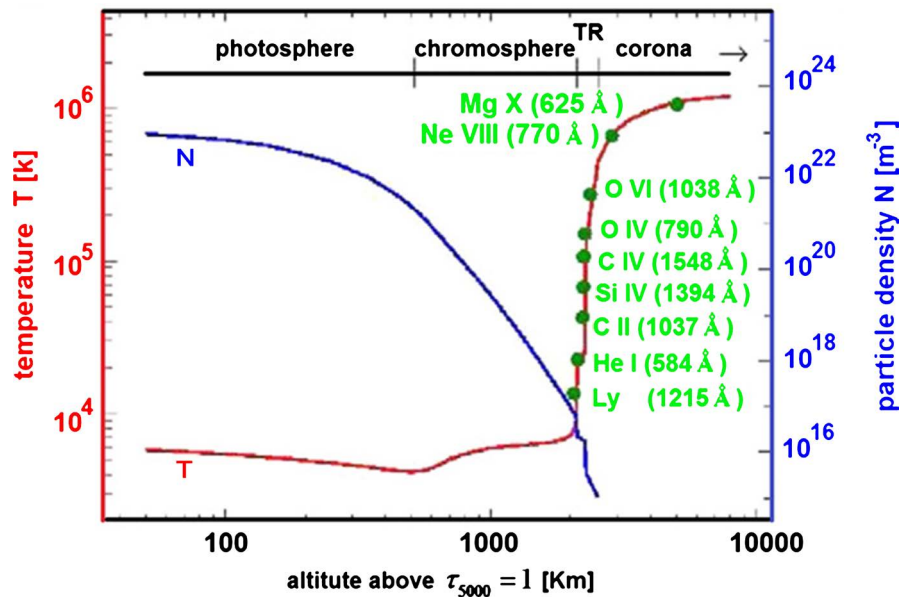


**Figure 2.** Height variations of the temperature and density of solar atmosphere. Adapted from H. Peter [46].

According to the standard model, the visible surface of the Sun, the photosphere, is the layer below which the Sun becomes opaque to visible light [43]. Above the photosphere visible sunlight is free to propagate into space, and almost all of its energy escapes the Sun entirely. The sunlight has the spectrum of a black-body radiating at about 5800 K.

Above the photosphere lies the chromosphere that is about 2500 km thick, dominated by a spectrum of emission and absorption lines. The temperature of the chromosphere increases gradually with altitude, ranging up to around 20,000 K near the top [47]. The particle density decreases rapidly from  $10^{22}$  to  $10^{17} \text{ m}^{-3}$ .

Above the chromosphere, in a thin (about 200 km) transition region, the temperature rises rapidly from around 20,000 K in the upper chromosphere to coronal temperatures closer to 1,000,000 K. The particle density decreases from  $10^{17}$  up to  $10^{16} - 10^{15} \text{ m}^{-3}$  in the low corona.

In our opinion, this is a zero level of the fractal structure. The calculated density according to (6.3) is:

$$\rho_f \cong 2.3 \times 10^{-9} \text{ kg/m}^3 \quad (6.4)$$

**Corona** is an aura of plasma that surrounds the Sun and other stars. The Sun's corona extends at least 8 million kilometers into outer space [48] and is most easily seen during a total solar eclipse. Spectroscopy measurements indicate strong ionization and plasma temperature in excess of 1,000,000 K [49]. The corona emits radiation mainly in the X-rays, observable only from space. The plasma is transparent to its own radiation and to that one coming from below, therefore we say that it is optically-thin. The gas, in fact, is very rarefied and the photon mean free-path overcomes by far all the other length-scales, including the typical sizes of the coronal features.

J. T. Schmelz has this to say about composition of Solar corona:

*Along with temperature and density, the elemental abundance is a basic parameter required by astronomers to understand and model any physical system. The abundances of the solar corona are known to differ from those of the solar photosphere [50].*

Wikipedia has this to say about the coronal heating problem:

*Coronal heating problem in solar physics relates to the question of why the temperature of the Sun's corona is millions of kelvins higher than that of the surface. The high temperatures require energy to be carried from the solar interior to the corona by non-thermal processes, because the second law of thermodynamics prevents heat from flowing directly from the solar photosphere (surface), which is at about 5800 K, to the much hotter corona at about 1 to 3 MK (parts of the corona can even reach 10 MK).*

In our opinion, the origin of the Solar corona plasma is not the coronal heating. Plasma particles (electrons, protons, multicharged ions) are so far apart that its temperature in the usual sense is not very meaningful. This plasma is the result of the annihilation of Dark Matter particles DMF1 with mass 1.3 TeV. The Solar corona resembles a honeycomb filled with plasma.

The following experimental results speak in favor of this model:

- The corona emits radiation mainly in the X-rays;
- The plasma is transparent to its own radiation and to that one coming from below;
- The abundances of the solar corona are known to differ from those of the solar photosphere;
- During the impulsive stage of Solar flares, radio waves, hard x-rays, and gamma rays with energy above 100 GeV are emitted (one photon emitted during the solar minimum had an energy as high as 467.7 GeV) [51];
- Assuming the particle density in the low corona  $10^{15} \text{ m}^{-3}$  and mass of DMF1:  $m_{DMF1} = 2.3 \times 10^{-24} \text{ kg}$  we can find mass density  $\rho_{DMF1}^{in} = 2.3 \times 10^{-9} \text{ kg/m}^3$  that is equal to the density of the fractal structure (6.4);
- A distance between particles DMF1 is about  $10^{-5} \text{ m}$  that is much smaller than the range of the weak interaction of DMPs  $R_W$  (4.1). It means that the Solar corona is a stable Shell around the Sun with density decreasing according to Equation (6.2) with inner radius about  $R_{in} \cong 7 \times 10^8 \text{ m}$  and outer radius  $R_{out}$ :

$$R_{out} = \frac{4\sigma_0/c^2}{m_{DMF1}n_{out}}$$

where  $n_{out}$  is the particle density of the Shell at the outer radius:

$n_{out} = R_W^{-3} = a^{-3} \times Q^{-3/4}$ . Considering this value of  $n_{out}$  we can calculate  $R_{out}$ :

$$R_{out} = 4\alpha^2 a \times Q^{3/4} \cong 3 \times 10^{12} \text{ m} \tag{6.5}$$

The total mass of the Shell  $M_{DMF1}$  is about:

$$M_{DMF1} = \frac{8\pi\sigma_0}{c^2} R_{out}^2 \cong 9 \times 10^{25} \text{ kg} \tag{6.6}$$

Observable outer radius of the Solar corona  $8 \times 10^9 \text{ m}$  [46] depends on the concentration of DMPs, the strength of their annihilation interaction, and a sensitivity of the measuring instrument.

**Geocorona.** According to Wikipedia,

*The geocorona is the luminous part of the outermost region of the Earth's atmosphere, the exosphere. It is seen primarily via far-ultraviolet light (Lyman-alpha) from the Sun that is scattered from neutral hydrogen. It extends to at least 15.5 Earth radii.*

Let's take a look at the structure of Earth atmosphere, its density and temperature depicted in **Figure 3**.

The atmosphere consists of five primary layers: the troposphere, stratosphere, mesosphere, thermosphere, and exosphere [53] [54] [55]:

- Troposphere: 0 to 12 km. It contains roughly 80% of the mass of Earth's atmosphere [56];
- Stratosphere: 12 to 50 km. The atmospheric pressure at the top of the stratosphere is roughly 1/1000 the pressure at sea level;
- Mesosphere: 50 to 80 km. The top of Mesosphere is the coldest place on Earth and has an average temperature around  $-85^\circ\text{C}$  [57] [58];

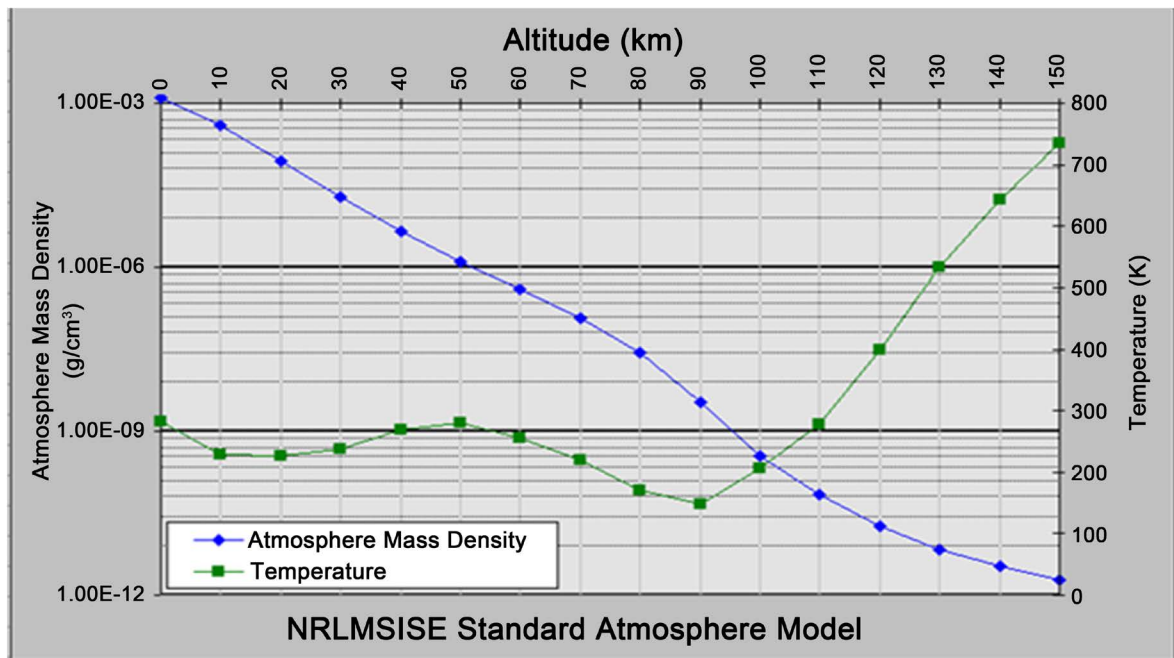


**Figure 3.** Temperature and mass density against altitude from NRLMSISE-00 standard atmosphere model. Adapted from M. Picone, A. E. Hedin, D. Drob [52].

- Thermosphere: 80 to 700 km. The highly diluted gas in this layer can reach 2500°C. The lower part of it, from 80 to 550 kilometers contains the ionosphere;
- Exosphere: 700 to 10,000 km. The top of exosphere merges into the solar wind.

The mesopause is the temperature minimum at the boundary between the mesosphere and the thermosphere. It consists of two minima—one at about 85 km and a stronger minimum at about 100 km [59] with temperatures below  $-143^{\circ}\text{C}$ .

**Far-ultraviolet photons in the exosphere** have been observed out to a distance of approximately 100,000 km from the Earth (15.5 Earth radii) [60]. The first high-quality and wide-field-of-view image of Earth's corona of 38 Earth radii (243,000 km) obtained by the first interplanetary microspacecraft [61].

The Hisaki satellite with the extreme ultraviolet spectrometer EXCEED acquires spectral images (52 - 148 nm) of the atmospheres/magnetospheres of planets from Earth orbit. Due to its low orbital altitude ( $\sim 1000$  km), the images taken by the instrument also contain the geocoronal emissions. In this context, EXCEED has provided quasi-continuous remote sensing observations of the geocorona with high temporal resolution ( $\sim 1$  min) since 2013 [62]. The most popular explanation of this geocoronal emission is the scattering of Solar Far-Ultraviolet (FUV) photons by exospheric hydrogen.

**X-rays from Earth's geocorona** were first detected by Chandra X-ray Observatory in 1999 [63]. X-rays were observed in the range of energies 0.08 - 10 keV [63]. The main mechanism explaining the geocoronal X-rays is that they are

caused by collisions between neutral atoms in the geocorona with carbon, oxygen and nitrogen ions that are streaming away from the Sun in the solar wind [63] [64] [65]. This process is called “charge exchange”, since an electron is exchanged between neutral atoms in geocorona and ions in the solar wind.

**X-rays from Planets** were also observed by Chandra [63]. According to NASA:

- *The X-rays from Venus and, to some extent, the Earth, are due to the fluorescence of solar X-rays striking the atmosphere;*
- *Fluorescent X-rays from oxygen atoms in the Martian atmosphere probe heights similar to those on Venus. A huge Martian dust storm was in progress when the Chandra observations were made. Since the intensity of the X-rays did not change when the dust storm rotated out of view, astronomers were able to conclude that the dust storm did not affect Mars's upper atmosphere;*
- *Jupiter has an environment capable of producing X-rays in a different manner because of its substantial magnetic field. X-rays are produced when high-energy particles from the Sun get trapped in its magnetic field and accelerated toward the polar regions where they collide with atoms in Jupiter's atmosphere. Chandra's image of Jupiter shows strong concentrations of X-rays near the north and south magnetic poles. The weak equatorial X-ray emission is likely due to reflection of solar X-rays;*
- *Like Jupiter, Saturn has a strong magnetic field, so it was expected that Saturn would also show a concentration of X-rays toward the poles. However, Chandra's observation revealed instead an increased X-ray brightness in the equatorial region. Furthermore, Saturn's X-ray spectrum, or the distribution of its X-rays according to energy, was found to be similar to that of X-rays from the Sun.*

V. I. Shematovich and D. V. Bisikalo gave the following explanation of the planetary coronas [66]:

*The measurements reveal that planetary coronas contain both a fraction of thermal neutral particles with a mean kinetic energy corresponding to the exospheric temperature and a fraction of hot neutral particles with mean kinetic energy much higher than the exospheric temperature. These suprathermal (hot) atoms and molecules are a direct manifestation of the non-thermal processes taking place in the atmospheres. These hot particles lead to the atmospheric escape, determine the coronal structure, produce non-thermal emissions, and react with the ambient atmospheric gas triggering hot atom chemistry.*

Let's summarize the obtained results for Geocorona and Planetary Coronas:

- FUV radiation has been observed out to a distance of approximately 243,000 km from the Earth;
- FUV radiation was observed in the wavelength range down to 52 nm;
- X-rays were observed in the range of energies 0.08 - 10 keV;
- X-rays from Venus are due to the fluorescence of solar X-rays striking the atmosphere;

- Fluorescent X-rays from oxygen atoms in the Martian atmosphere probe heights similar to those on Venus. Dust storm did not affect Mars's upper atmosphere;
- Jupiter's X-rays are produced when high-energy particles from the Sun get trapped in its magnetic field and accelerated toward the polar regions where they collide with atoms in Jupiter's atmosphere;
- Saturn's X-ray spectrum was found to be similar to that of X-rays from the Sun;
- Suprathermal (hot) atoms and molecules are a direct manifestation of the non-thermal processes taking place in the atmospheres. These hot particles produce non-thermal emissions.

In our opinion, the described picture of Geo and Planetary Coronas is similar to the picture of the Solar Corona:

- The Earth thermosphere and exosphere composed of DMF1 explains the difference in the size of the Geocorona and the size of the Earth: The Sun and Solar corona have the same ratio of sizes;
- At the distance of 243,000 km from the Earth, atoms and molecules are so far apart that they can travel hundreds of kilometers without colliding with one another. Thus, the exosphere no longer behaves like a gas, and the particles constantly escape into space. In our view, FUV radiation and X-rays are the consequence of DMF1 annihilation;
- All planets and some observed satellites (Europa, Io, Io Plasma Torus, Titan) have X-rays in upper atmosphere of the planets, similar to the Solar Corona;
- The calculated density of the Earth's fractal structure  $\rho_f \cong 2.5 \times 10^{-7} \text{ kg/m}^3$  (6.3) is in good agreement with experimental results for atmosphere density at the lowest temperature (below  $-143^\circ\text{C}$ ) at 100 km altitude, similar to that of the Solar Corona;
- The most impressive result is that Saturn's X-ray spectrum is similar to that of X-rays of the Sun;
- Suprathermal atoms and molecules proposed by V. I. Shematovich and D. V. Bisikalo are the result of DMF1 annihilation in Geocorona, similar to that of Solar corona.

We suppose that not only gravitationally-rounded objects in the Solar System have Coronas made up of Dark Matter particles, but so do all gravitationally-rounded Macroobjects of the World.

## 7. Conclusions

Dark Matter is abundant:

- 2.4% of Light Matter is in Superclusters, Galaxies, Stars, Planets, etc.
- 4.8% of Light Matter is in the Medium of the World;
- The remaining 92.8% of mass is Dark Matter.

Dark Matter is omnipresent:

- Dark Matter Reactors in Cores of all gravitationally-rounded Macroobjects;

- Coronas of all Macroobjects of the World;
- The Medium of the World.

In the present paper, we develop the Rotational Fission model of creation and evolution of Macrostructures of the World (Superclusters, Galaxies, Extrasolar Systems), based on Overspinning Cores of the World's Macroobjects, and the Law of Conservation of Angular Momentum. To be consistent with this Fundamental Law, we develop New Physics of the World:

- The main players of the World are overspinning Dark Matter Cores of Superclusters;
- Milky Way galaxy was born 13.8 billion years ago as the result of a Gravitational Burst of the Local Supercluster Core due to its rotational fission;
- Proposed Fifth Fundamental force of Weak Interaction between Dark Matter particles provides the integrity of Dark Matter Cores of all Macroobjects;
- Proposed new Dark Matter particles Dions with mass 0.2 eV compose outer Shell of Supercluster's Cores and are responsible for the gravitational interaction.

It is time to adopt the existence of the Dark Matter in the World from the Classical Physics point of view.

## Acknowledgements

Special thanks to my son Ilya Netchitailo, who questioned every aspect of the Model, gave valuable suggestions and helped shape it to its present form.

## Conflicts of Interest

The author declares no conflicts of interest regarding the publication of this paper.

## References

- [1] Netchitailo, V. (2016) Overview of Hypersphere World-Universe Model. *Journal of High Energy Physics, Gravitation and Cosmology*, **2**, 593-632. <https://doi.org/10.4236/jhepgc.2016.24052>
- [2] Swedenborg, E. (1734) Latin: Opera Philosophica et Mineralia (English: Philosophical and Mineralogical Works). Principia, 1. [http://www.swedenborg.org.uk/bookshop/swedenborg\\_a-z/the\\_principia\\_2\\_vols](http://www.swedenborg.org.uk/bookshop/swedenborg_a-z/the_principia_2_vols)
- [3] Baker, G.L. (1983) Emanuel Swedenborg—An 18th Century Cosmologist. *The Physics Teacher*, 441. <http://www.newchurchhistory.org/articles/glb2007/baker.pdf> <https://doi.org/10.1119/1.2341354>
- [4] Brush, S.G. (2014) A History of Modern Planetary Physics: Nebulous Earth. 7.
- [5] Ferrell, V. (1996) The Wonders of Nature. Harvestime Books, Altamont.
- [6] Darwin, G.H. (1879) On the Bodily Tides of Viscous and Semi-Elastic Spheroids, and on the Ocean Tides upon a Yielding Nucleus. *Philosophical Transactions of the Royal Society*, **170**, 1. <https://doi.org/10.1098/rstl.1879.0061>
- [7] Wise, D.U. (1966) Origin of the Moon by Fission. <http://adsabs.harvard.edu/full/1966ems..conf..213W>

- [8] Jacot, L. (1986) Heretical Cosmology (Transl. of Science et bon sense, 1981). Exposition-Banner.
- [9] Van Flandern, T. (1999) Dark Matter, Missing Planets, and New Comets. North Atlantic.
- [10] Netchitailo, V. (2015) 5D World-Universe Model. Multicomponent Dark Matter. *Journal of High Energy Physics, Gravitation and Cosmology*, **1**, 55-71. <https://doi.org/10.4236/jhepgc.2015.12006>
- [11] Netchitailo, V. (2017) Astrophysics: Macroobject Shell Model. *Journal of High Energy Physics, Gravitation and Cosmology*, **3**, 776-790. <https://doi.org/10.4236/jhepgc.2017.34057>
- [12] Netchitailo, V. (2018) Hypersphere World-Universe Model. Tribute to Classical Physics. *Journal of High Energy Physics, Gravitation and Cosmology*, **4**, 441-470. <https://doi.org/10.4236/jhepgc.2018.43024>
- [13] NASA (2015) The Cosmic Distance Scale. [https://imagine.gsfc.nasa.gov/features/cosmic/local\\_supercluster\\_info.html](https://imagine.gsfc.nasa.gov/features/cosmic/local_supercluster_info.html)
- [14] Tully, R.B. (1982) The Local Supercluster. *Astrophysical Journal*, **257**, 389.
- [15] Ness, M., *et al.* (2015) The Cannon: A Data-Driven Approach to Stellar Label Determination. *The Astrophysical Journal*, **808**, 1. <https://doi.org/10.1088/0004-637X/808/1/16>
- [16] Heymans, C., *et al.* (2008) The Dark Matter Environment of the Abell 901/902 Supercluster: A Weak Lensing Analysis of the HST STAGES Survey.
- [17] Zwicky, F. (1933) Die Rotverschiebung von extragalaktischen Nebeln. *Helvetica Physica Acta*, **6**, 110.
- [18] Marchetti, T., Rossi, E.M. and Brown, A.G.A. (2018) *Gaia* DR2 in 6D: Searching for the Fastest Stars in the Galaxy. *Monthly Notices of the Royal Astronomical Society*, sty2592. <https://doi.org/10.1093/mnras/sty2592>
- [19] Clarke, C.J., *et al.* (2018) High-Resolution Millimeter Imaging of the CI Tau Protoplanetary Disk: A Massive Ensemble of Protoplanets from 0.1 to 100 au. *The Astrophysical Journal Letters*, **866**, L6. <https://doi.org/10.3847/2041-8213/aae36b>
- [20] Djorgovski, S.G. (2016) Stellar Structure and the Sun. [http://www.astro.caltech.edu/~george/ay1/lec\\_pdf/Ay1\\_Lec08.pdf](http://www.astro.caltech.edu/~george/ay1/lec_pdf/Ay1_Lec08.pdf)
- [21] Dziewonski, A.M. and Anderson, D.L. (1981) Preliminary Reference Earth Model. *Physics of the Earth and Planetary Interiors*, **25**, 297-356.
- [22] Turcotte, D.L. and Schubert, G. (2002) Geodynamics. Cambridge University Press, Cambridge, 137. <https://doi.org/10.1017/CBO9780511807442>
- [23] Pollack, H.N., Hurter, S.J. and Johnson, J.R. (1993) Heat Flow from the Earth's Interior: Analysis of the Global Data Set. *Reviews of Geophysics*, **31**, 267-280. <https://doi.org/10.1029/93RG01249>
- [24] Arculus, R. (2016) The Cosmic Origins of Uranium. <http://www.world-nuclear.org/information-library/nuclear-fuel-cycle/uranium-resources/the-cosmic-origins-of-uranium.aspx>
- [25] Gando, A., *et al.* (2011) Partial Radiogenic Heat Model for Earth Revealed by Geoneutrino Measurements. *Nature Geoscience*, **4**, 647-651. <https://doi.org/10.1038/ngeo1205>
- [26] Hoffman, D.C., *et al.* (1971) Detection of Plutonium-244 in Nature. *Nature*, **234**, 132-134. <https://doi.org/10.1038/234132a0>
- [27] Ricard, Y. (2009) Physics of Mantle Convection. In: Bercovici, D. and Schubert, G.,

- Eds., *Treatise on Geophysics: Mantle Dynamics*, Vol. 7, Elsevier Science, Amsterdam, 2.
- [28] Cole, G.H.A. and Woolfson, M.M. (2002) Planetary Science: The Science of Planets around Stars. Institute of Physics Publishing, 36-37, 380-382.  
<https://doi.org/10.1201/9781420056853>
- [29] Kinver, M. (2009) Global Average Temperature May Hit Record Level in 2010. BBC.
- [30] Elkins-Tanton, L.T. (2006) Jupiter and Saturn. Chelsea House, New York.
- [31] O'Donoghue, J., Moore, L., Stallard, T.S. and Melin, H. (2016) Heating of Jupiter's Upper Atmosphere above the Great Red Spot. *Nature*, **536**, 190-192.  
<https://doi.org/10.1038/nature18940>
- [32] De Pater, I. and Lissauer, J.J. (2010) Planetary Sciences. Cambridge University Press, Cambridge, 2nd Edition, 254-255.  
<https://doi.org/10.1017/CBO9780511780561>
- [33] (2004) Class 12—Giant Planets—Heat and Formation. 3750—Planets, Moons & Rings. Colorado University, Boulder.
- [34] Pearl, J.C. and Conrath, B.J. (1991) The Albedo, Effective Temperature, and Energy Balance of Neptune, as Determined from Voyager Data. *Journal of Geophysical Research: Space Physics*, **96**, 18921-18930.
- [35] Goddard Space Flight Center (2010) Goddard Instrument Aboard Cassini Spacecraft Sees "Pac-Man" on Saturn Moon.  
<https://www.nasa.gov/centers/goddard/news/features/2010/pac-man-mimas.html>
- [36] Fossat, E., *et al.* (2017) Asymptotic g Modes: Evidence for a Rapid Rotation of the Solar Core. arXiv:1708.00259.
- [37] Zhang, J., *et al.* (2005) Inner Core Differential Motion Confirmed by Earthquake Waveform Doublets. *Science*, **309**, 1357-1360.  
<https://doi.org/10.1126/science.1113193>
- [38] Guillot, T., *et al.* (2018) A Suppression of Differential Rotation in Jupiter's Deep Interior. *Nature*, **555**, 227-230. <https://www.nature.com/articles/nature25775>  
<https://doi.org/10.1038/nature25775>
- [39] Feulner, G. (2012) The Faint Young Sun Problem. arXiv:1204.4449.  
<https://doi.org/10.1029/2011RG000375>
- [40] Hoyle, F. (1958) Remarks on the Computation of Evolutionary Tracks. *Ricerche Astronomiche*, **5**, 223.
- [41] Schwarzschild, M. (1958) Structure and Evolution of the Stars. Princeton University Press, Princeton. <https://doi.org/10.1515/9781400879175>
- [42] Newman, M.J. and Rood, R.T. (1977) Implications of Solar Evolution for the Earth's Early Atmosphere. *Science*, **198**, 1035-1037.  
<https://doi.org/10.1126/science.198.4321.1035>
- [43] Gough, D.O. (1981) Solar Interior Structure and Luminosity Variations. *Solar Physics*, **74**, 21-34. <https://doi.org/10.1007/BF00151270>
- [44] Baryshev, Yu. (2008) Field Fractal Cosmological Model as an Example of Practical Cosmology Approach. arXiv:0810.0162.
- [45] Agle, D.C. and Brown, D. (2012) Data from NASA's Voyager 1 Point to Interstellar Future. [http://www.nasa.gov/mission\\_pages/voyager/voyager20120614.html](http://www.nasa.gov/mission_pages/voyager/voyager20120614.html)
- [46] Peter, H. (2004) Structure and Dynamics of the Low Corona of the Sun. *Reviews in Modern Astronomy*, **17**, 87.

- [47] Abhyankar, K.D. (1977) A Survey of the Solar Atmospheric Models. *Bulletin of the Astronomical Society of India*, **5**, 40.
- [48] Fox, K.C. (2014) NASA's STEREO Maps Much Larger Solar Atmosphere than Previously Observed.  
<https://www.nasa.gov/content/goddard/nasas-stereo-maps-much-larger-solar-atmosphere-than-previously-observed/>
- [49] Aschwanden, M.J. (2004) Physics of the Solar Corona. An Introduction. Praxis Publishing.
- [50] Schmelz, J.T., *et al.* (2012) Composition of the Solar Corona, Solar Wind, and Solar Energetic Particles. *The Astrophysical Journal*, **755**, 33.  
<http://iopscience.iop.org/article/10.1088/0004-637X/755/1/33/pdf>  
<https://doi.org/10.1088/0004-637X/755/1/33>
- [51] Grossman, L. (2018) Strange Gamma Rays from the Sun May Help Decipher Its Magnetic Fields. *Science News*, **194**, 9.  
<https://www.sciencenews.org/article/strange-gamma-rays-sun-magnetic-fields>
- [52] Picone, M., Hedin, A.E. and Drob, D. (2017) NRL MSISE-00 (Mass Spectrometer Incoherent Scatter) Model of the Upper Atmosphere.  
<https://www.ukssdc.ac.uk/wdcc1/nrlmsise00.html>
- [53] Zell, H. (2015) Earth's Upper Atmosphere. NASA.  
[https://www.nasa.gov/mission\\_pages/sunearth/science/mos-upper-atmosphere.html](https://www.nasa.gov/mission_pages/sunearth/science/mos-upper-atmosphere.html)
- [54] Russell, R. (2008) The Thermosphere. Windows to the Universe.  
<https://www.windows2universe.org/?page=/earth/Atmosphere/thermosphere.html>
- [55] Geerts, B. and Linacre, E. (1997) The Height of the Tropopause.  
<http://www-das.uwyo.edu/~geerts/cwx/notes/chap01/tropo.html>
- [56] Troposphere (1984) Concise Encyclopedia of Science & Technology. McGraw-Hill, New York.
- [57] States, R.J. and Gardner, C.S. (2000) Thermal Structure of the Mesopause Region (80-105 km) at 40 °N Latitude. Part I: Seasonal Variations. *Journal of the Atmospheric Sciences*, **57**, 66.
- [58] Buchdahl, J. (2010) Atmosphere, Climate & Environment Information Programme.  
<http://www.ace.mmu.ac.uk/eae/atmosphere/older/mesosphere.html>
- [59] Xu, J., *et al.* (2007) Mesopause Structure from Thermosphere, Ionosphere, Mesosphere, Energetics, and Dynamics (TIMED)/Sounding of the Atmosphere Using Broadband Emission Radiometry (SABER) Observations. *Journal of Geophysical Research*, **112**, D9.  
<https://agupubs.onlinelibrary.wiley.com/doi/full/10.1029/2006JD007711>
- [60] Reyes, R. Exploring the Sun-Earth Connection. Southwest Research Institute.  
<http://pluto.space.swri.edu/image/glossary/geocorona.html>
- [61] Kameda, S., *et al.* (2017) Ecliptic North-South Symmetry of Hydrogen Geocorona. *Geophysical Research Letter*, **44**, Article ID: 11706.  
<https://doi.org/10.1002/2017GL075915>
- [62] Kuwabara, M., *et al.* (2017) The Geocoronal Responses to the Geomagnetic Disturbances. *Journal of Geophysical Research: Space Physics*, **122**, 1269-1276.  
<https://agupubs.onlinelibrary.wiley.com/doi/pdf/10.1002/2016JA023247>
- [63] NASA (2012) Solar System.  
[http://chandra.harvard.edu/xray\\_sources/solar\\_system.html](http://chandra.harvard.edu/xray_sources/solar_system.html)
- [64] Wargelin, B.J., *et al.* (2014) Observation and Modeling of Geocoronal Charge Exchange X-Ray Emission during Solar Wind Gusts. *The Astrophysical Journal*, **796**,

28. <https://doi.org/10.1088/0004-637X/796/1/28>

[65] Cravens, T.E., *et al.* (2009) Solar Wind Charge Exchange Contributions to the Diffuse X-Ray Emission. *AIP Conference Proceedings*, **1156**, 37-51.

<https://doi.org/10.1063/1.3211832>

[66] Shematovich, V.I. and Bisikalo, D.V. (2018) Hot Planetary Coronas. *Planetary Science*.

<http://planetaryscience.oxfordre.com/view/10.1093/acrefore/9780190647926.001.0001/acrefore-9780190647926-e-104>